

## EVIDENCE FOR A GALACTIC SUNYAEV-ZEL'DOVICH-LIKE SIGNAL IN WMAP DATA

SHAHAB JOUDAKI, JOSEPH SMIDT, ALEXANDRE AMBLARD, AND ASANTHA COORAY  
 Center for Cosmology, Department of Physics and Astronomy, University of California, Irvine, CA 92697  
*Draft version March 3, 2019*

### ABSTRACT

The Sunyaev-Zel'dovich (SZ) effect has a distinct spectral signature that allows its separation from fluctuations in the cosmic microwave background (CMB) and foregrounds. Using CMB anisotropies measured in Wilkinson Microwave Anisotropy Probe's five-year maps, we constrain the SZ fluctuations at large, degree angular scales corresponding to multipoles in the range from 10 to 400. While we do not find any evidence for SZ fluctuations at multipoles greater than 50, we do find evidence for an SZ-like signal at ten degrees angular scales. We have failed to explain it as a residual from known Galactic foregrounds. If this signal is in fact the SZ effect associated with electrons of  $\sim 1$  keV in the outskirts of the Galactic halo, the required column density of electrons is  $\sim 1.5 \times 10^{22} \text{ cm}^{-2}$ . The ten degrees angular scale SZ signal is consistent with the FIRAS bound on the CMB spectral distortions.

### 1. INTRODUCTION

The Sunyaev-Zel'dovich (SZ) effect (Sunyaev & Zel'dovich 1972) is the inverse Compton scattering of the cosmic microwave background (CMB) by electrons throughout the universe. The SZ effect can be partitioned into two components: the kinetic effect (also known as the Ostriker-Vishniac effect; Ostriker & Vishniac 1986) due to bulk motion of electrons with respect to the rest frame of the microwave background, and the thermal effect due to energy transfer from hot electrons in massive galaxy clusters (Komatsu & Kitayama 1999; Springel et al. 2001; Cooray 2000; Molnar & Birkinshaw 2000; Seljak et al. 2001; Sadeh & Rephaeli 2004). The SZ thermal signal is expected to be important in future constraints on the underlying cosmology of the universe, by revealing the properties of clusters in cluster-counting experiments (e.g. see Carlstrom et al. 2002) and via the angular power spectrum (Komatsu & Seljak 2002).

While the first-generation arcminute angular scale experiments found a large amplitude for the SZ power spectrum (Sievers et al. 2009; Reichardt et al. 2008; Dawson et al. 2006; Sharp et al. 2009; Friedman et al. 2009; Sayers et al. 2008), more recent results from South Pole Telescope (Lueker et al 2009) and Atacama Cosmology Telescope (Fowler et al 2010) find an amplitude that is lower than expected in the standard cosmological model. At degree angular scales, there are no detections of the SZ fluctuations as primordial anisotropies of the CMB dominate the SZ signal by at least 3 orders of magnitude. Fortunately, a separation of the SZ anisotropies from those of CMB is possible due to the fact that the SZ effect has a distinct frequency spectrum, as the inverse-Compton scattering on average increases the net energy of the CMB photons and move photons from the low frequency Rayleigh-Jeans (RJ) tail to higher frequencies (Sunyaev & Zel'dovich 1972). In multi-frequency CMB experiments spanning a wide range of frequency coverage across the SZ null frequency at 217 GHz, one can separate the CMB down to sub-percent level required to study the SZ anisotropy power spectrum (Cooray et al. 2000). This approach was first applied to constrain the sub-degree SZ fluctuations in BOOMERanG 2003 data (Veneziani et al 2009). Here, we analyze the WMAP five-

year CMB data to constrain SZ anisotropies at degree angular scales corresponding to multipoles  $\ell = 10 - 400$  on the sky. We ignore  $\ell < 10$  due to large uncertainties associated with simulating the CMB sky properly to match WMAP data at these multipoles.

In Section 2 we detail our approach to extract the SZ signal from the multifrequency WMAP5 data set; in Section 3 we present our results; and in Section 4 we provide a discussion of these results.

### 2. CMB AND FOREGROUND REMOVAL

We distinguish the SZ signal from other sources of anisotropies by minimizing the covariance relative to the SZ frequency dependence (also see Veneziani et al 2009). Although this technique is originally employed for removing foregrounds from CMB anisotropies (Tegmark & Efstathiou 1996; Tegmark et al. 2003; Amblard et al. 2007), we utilize it to recover SZ fluctuations, from which the primordial CMB is subtracted along with other sources of noise.

Thus, we obtain the raw SZ power spectrum from a weighted mean of the spectra in different frequency bands via (Cooray et al 2000):

$$C_{\ell}^{\text{rawSZ}} = \mathbf{w}_{\ell}^T \mathbf{C}_{\ell} \mathbf{w}_{\ell}, \quad (1)$$

where the scale dependent weights  $\mathbf{w}_{\ell}$  at each frequency can be obtained by minimizing the covariance  $\mathbf{C}$  of the multipole moments  $a_{\ell m}$ .

We enforce the constraint that SZ estimation is unbiased, via  $\sum_i w_{\ell}(\nu_i) = 1$ . The optimal weights for reconstructing the SZ are obtained from the covariance matrix:

$$\mathbf{w}_{\ell} = \frac{\mathbf{C}_{\ell}^{-1} \mathbf{e}}{\mathbf{e}^T \mathbf{C}_{\ell}^{-1} \mathbf{e}}, \quad (2)$$

where  $\mathbf{e}$  is a unit vector, such that  $e(\nu_i) = 1 \forall \nu_i$ .

We further construct the covariance matrix in frequency bands  $i$  and  $j$  as a function of angular scale:

$$\mathbf{C}_{(ij)}(\ell) = \frac{\langle a_{\ell m}^i a_{\ell m}^{j*} \rangle}{f_{\text{sky}} s(\nu_i) s(\nu_j)}, \quad (3)$$

where  $s(\nu_i)$  is the SZ frequency dependence at the center of each of the WMAP frequency bands relative

to the CMB, with  $s(\nu) = 2 - (x/2)\coth(x/2)$ ,  $x = h\nu/kT_{\text{CMB}} \approx \nu/56.8$  GHz. In the RJ limit  $s(\nu) \rightarrow 1$ , such that  $C_\ell^{\text{SZ}}(\nu, \nu') = s(\nu)s(\nu')C_\ell^{\text{SZ}}$ , where  $C_\ell^{\text{SZ}}$  is the SZ power spectrum in the RJ limit. For the two preferred WMAP5 bands [V, W] = [60.8, 93.5] GHz, we find  $s(\nu) = [0.906, 0.784]$ . For the data, the multipole moments are obtained from WMAP five-year maps

$$a_{\ell m}^{\text{data}} = a_{\ell m}^{\text{WMAP}}/b_\ell, \quad (4)$$

normalized by the measured beam window function in the respective frequency band. In Figure 1, we illustrate the power spectrum of the W-band map from WMAP5 and compare it to simulations described below.

To compute the covariance matrix, we simulated a set of 250 Gaussian sky maps with HEALPix<sup>1</sup> based on the CAMB-generated (Lewis et al 1999) input power spectrum in accordance with the WMAP5 best-fit  $\Lambda$ CDM cosmology ( $[\Omega_c h^2, \Omega_b h^2, \Omega_\Lambda, n_s, \tau, \Delta_R^2] = [0.1099, 0.02273, 0.742, 0.963, 0.087, 2.41 \times 10^{-9}]$ ). We also found consistent results when generating simulations using the exact WMAP-5 measured CMB power spectrum in each of the bands. From these frequency independent maps, masked along the Galactic plane via KQ75 (admitting 71.8% of the sky), we then produced the moments  $a_{\ell m}^G$  up to  $\ell = 400$  with HEALPix. To account for the masking in our estimated spectra, we used the algorithm described by Hivon et al (2002).

In addition to these CMB simulations, we created 250 noise maps for each frequency band, given by

$$N_\nu(\hat{\mathbf{n}}) = \frac{\sigma_{0;\nu}}{\sqrt{N_{\text{obs};\nu}}} n(\hat{\mathbf{n}}), \quad (5)$$

where  $N_\nu(\hat{\mathbf{n}})$  is the noise map,  $n(\hat{\mathbf{n}})$  is a white noise map, the frequency dependent  $N_{\text{obs}}$  is the number of observations per pixel, and the noise per observation  $\sigma_0 = [3.133, 6.538]$  mK for the [V, W] bands<sup>2</sup>. From these maps, we produce the noise multipole moments,  $a_{\ell m}^N$ , out to the same angular scale as their CMB counterparts. We correct for the frequency dependent beam transfer function,  $b_\ell$ , by adding the CMB and noise simulations according to  $a_{\ell m} = a_{\ell m}^G + a_{\ell m}^N/b_\ell$ .

In order to estimate the SZ signal, we compared these simulations to WMAP5 data, which represent a weighted mean of the five single-year maps (Gold et al 2009). In subtracting from the unreduced maps synchrotron and free-free emission, primarily at frequencies below 60 GHz, and thermal dust emission which dominates at frequencies above 60 GHz, the WMAP team (Hinshaw et al 2007, Page et al 2007, Gold et al 2009) utilized an offset-subtracted map of Haslam et al (1982), an extinction-corrected H $\alpha$  map of Finkbeiner (2003), and dust emission Model 8 of Finkbeiner et al (1999).

We have accounted for the potential of systematic uncertainties in the WMAP team's foreground removal by adding to the multipole moments of the CMB and noise simulations a contribution from foreground residuals. In our analysis, we further considered 1% uncertainties in the beam transfer functions of each frequency band (Hill et al 2009). Thus, the multipole moments from simula-

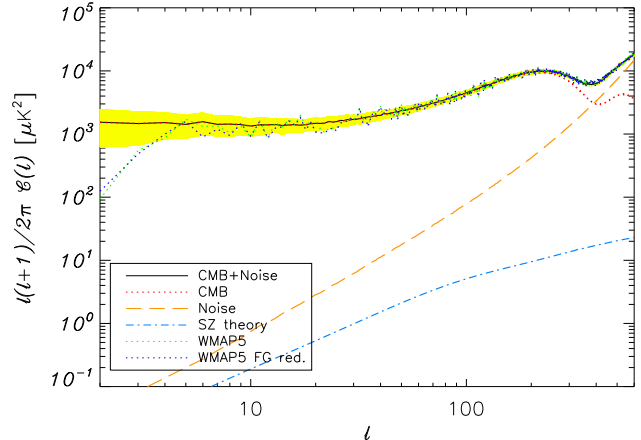


FIG. 1.— The average simulated auto spectrum in the W frequency band for the combination of Gaussian CMB and noise is illustrated by a black solid line about its  $1\sigma$  yellow error band. The red dotted line is the contribution from the CMB alone and the red dashed line represents the contribution from the noise. The blue and green dotted lines illustrate the spectra obtained from the foreground reduced and unreduced WMAP5 maps, respectively. The dot-dashed blue line represents the signal from the theoretical Komatsu-Seljak SZ power spectrum (Komatsu & Seljak 2002).

tions take on the final combined form

$$a_{\ell m}^{\text{sim}} = a_{\ell m}^G + a_{\ell m}^N/(b_\ell + B_\nu(\ell)) + a_{\ell m}^d D_\nu + a_{\ell m}^{\text{ff}} F_\nu + a_{\ell m}^{\text{sync}} S_\nu, \quad (6)$$

where  $B_\nu(\ell) = \Delta b_b \gamma_b(\ell)$ ,  $D_\nu = \Delta b_d \gamma_d$ ,  $F_\nu = \Delta b_{ff} \gamma_{ff}$ , and  $S_\nu = \Delta b_{\text{sync}} \gamma_{\text{sync}}$ , such that  $\gamma$  is a frequency dependent, but multipole independent unless otherwise specified, Gaussian random number drawn for each of the 250 simulations. The  $\Delta b$  quantities encapsulate a 1% uncertainty in the beams, and a [4.4, 5.6]% uncertainty on the amplitudes of the considered dust, free-free, and synchrotron foreground templates in the [V, W] bands. The synchrotron foreground template was constructed by the difference of the WMAP5 temperature map in

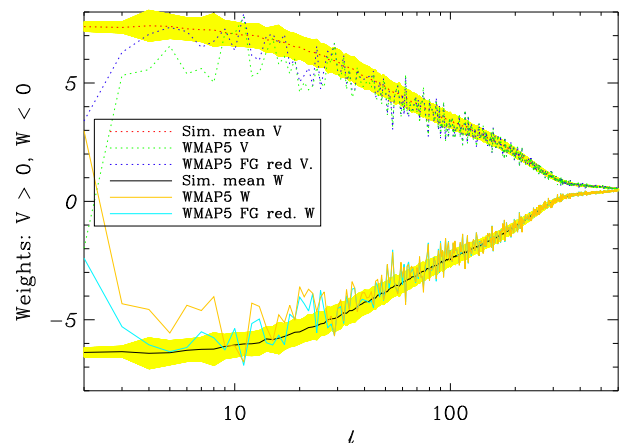


FIG. 2.— Optimal weights constructed from the covariance matrix following Eqn. 2. The upper set of dotted lines are obtained from the V-band and the lower set of solid lines from the W-band. The mean simulated weights run through the yellow bands, representing the  $1\sigma$  uncertainty about the mean. The foreground cleaned and uncleaned weights from WMAP5 are also illustrated for each frequency band.

<sup>1</sup> <http://healpix.jpl.nasa.gov>

<sup>2</sup> <http://lambda.gsfc.nasa.gov/product/map/dr3/>

the K band (22.8 GHz) with that of the Ka band (33.0 GHz), whereas the other two templates were obtained from the LAMBDA<sup>2</sup> website. The frequency dependent amplitudes are given in Table 2 of Gold et al (2009). The uncertainties on the foreground templates were obtained from the stated 15  $\mu\text{K}$  uncertainty on the removal of the combined foregrounds (Gold et al 2009). As shown in Table 3, the foregrounds render a bias and increase the uncertainty in the SZ estimation primarily on large scales ( $\ell < 50$ ), whereas the uncertainty in the beam window functions has the corresponding effect dominantly on smaller scales.

In addition to our account of residual foregrounds in the error analysis, we add a flat spectrum of radio point sources to the temperature power spectrum of the above simulations, such that  $C_\ell^{\text{TT}} \rightarrow C_\ell^{\text{G+N+FG}_{\text{res}}} + C_\ell^{\text{ps}}$ , via the frequency dependent model for the point source power spectrum (Nolta et al 2009)

$$C_\ell^{\text{ps}}(\nu_i, \nu_j) = A_{\text{ps}} r(\nu_i) r(\nu_j) \left( \frac{\nu_i \nu_j}{\nu_Q^2} \right)^{\alpha-2}, \quad (7)$$

where  $\nu_i$  and  $\nu_j$  are the central frequencies of the two considered bands, normalized by that of the Q band  $\nu_Q = 40.7$  GHz,  $A_{\text{ps}}$  is the point source amplitude, and  $\alpha = -0.09$  is the spectral index of the point source flux. Moreover,

$$r(\nu) = \frac{(e^x - 1)^2}{x^2 e^x} \quad (8)$$

such that  $x \equiv h\nu/kT_{\text{CMB}}$ . The point source amplitude takes on the value  $(11.1 \pm 4.1) \times 10^{-3} \mu\text{K}^2\text{sr}$  for the frequency band combination VW (Nolta et al 2009). In addition to point source removal, we account for the uncertainty in the amplitude and spectral index. In Table 3 we see that point sources primarily bias our results on small scales.

The multipole ranges for our bins are listed in Table 3. We obtain the binned spectra by weighting each  $C_\ell$  (for the case of the simulations the spectra are averaged over the 250 simulations) with the respective uncertainty  $\sigma_\ell$  at that multipole.

### 3. RESULTS

We show the contributions to the power spectrum from the CMB, noise, and their combination, along with the WMAP five-year spectrum and the theoretical Komatsu-Seljak SZ power spectrum (2002) for the W band in Fig. 1. The WMAP data trace the simulated spectra closely, which become shot noise dominated at multipoles  $\ell > 350$ .

In Table 3, we state the binned weights of the foreground reduced WMAP5 data for the two frequency bands. The optimal weights at each multipole are illustrated in Fig. 2 for both the data and simulations. The two bands have weights roughly symmetrically aligned along zero, and decrease towards smaller angular scales. The residuals are the average spectra measured on our SZ-free simulations and represent our bias. The total residual is slightly different from the sum of the partial residuals due to correlation between components. The uncertainties in the table are the  $2\sigma$  dispersion  $\sigma_{\text{bin}}$  measured with our simulations. The final SZ spectrum val-

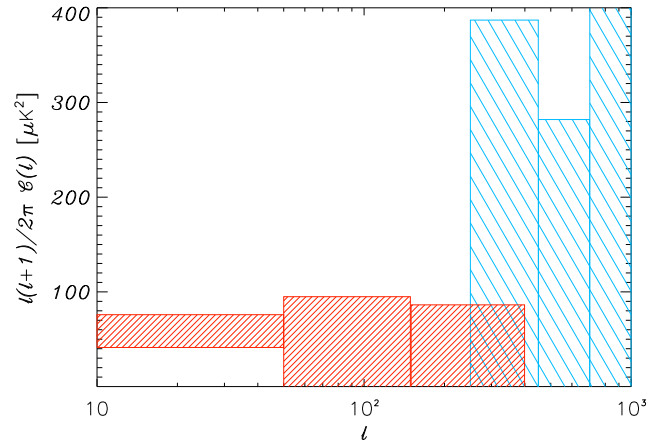


FIG. 3.— 95%-level constraints on the SZ signal in the power spectrum from WMAP five-year data in the [V, W] frequency bands (thinly-sliced red bars), along with smaller scale BOOMERanG 2003 data in thickly-sliced blue bars from Veneziani et al (2009).

TABLE 1. SZ POWER SPECTRUM ESTIMATES

	Bin 1	Bin 2	Bin 3
$\ell$ -range	10 – 50	50 – 150	150 – 400
Optimal weights			
$w_{60.8\text{GHz}}$	5.95	3.69	1.08
$w_{93.5\text{GHz}}$	-4.95	-2.69	-0.0831
Raw SZ	259	1740	4860
Residuals			
CMB & Noise	139	1650	4690
Foregrounds	57.4	26.7	35.5
Beam	-0.0414	-0.754	7.97
Point sources	3.08	21.9	77.5
Total residual	201	1700	4810
SZ Band Power Uncertainties			
CMB & Noise	15.5	50.3	49.7
Foregrounds	7.47	1.82	0.948
Beam	0.912	2.00	4.63
Point sources	0.933	3.75	5.85
Final SZ Power	$58.6 \pm 17.3$	$44.4 \pm 50.5$	$36.0 \pm 50.3$

The table derives the SZ angular power spectrum  $\ell(\ell+1)C_\ell/2\pi$  at the RJ end of the frequency spectrum. All values are tabulated in units of  $\mu\text{K}^2$ , except for the unitless weights. The scale-dependent weights and Raw SZ spectrum (foreground unreduced) are both measured from data, whereas we simulate the contribution from the CMB, instrumental noise, beam error, and point source error. The data maps are foreground cleaned by the WMAP team, but we account for potential residual foregrounds in our analysis. The uncertainties are given at the 95% c.l.

ues are corrected from the residual bias. The total error budget is given by the rms of the partial uncertainties.

In Fig. 3 we show our final estimate of the SZ-like power spectrum in distinct multipole bins for a combination of the [V, W] bands. There seems to be a clear non-zero signal at the largest angular scales ( $10 < \ell < 50$ ). Although foregrounds have already been reduced, this SZ signal could potentially be due to further systematic uncertainties in the foreground removal. The limits on the SZ signal from a 2003 BOOMERanG flight (Masi et al 2006, Veneziani et al 2009) have been included for comparison. In addition, if we modify Eqn. 1 from  $C_\ell^{\text{rawSZ}} = \mathbf{w}_\ell^T \mathbf{C}_\ell \mathbf{w}_\ell$  to include a noise-subtraction, such that  $C_\ell^{\text{rawSZ}} = \mathbf{w}_\ell^T (\mathbf{C}_\ell - \langle \mathbf{N}_\ell \rangle) \mathbf{w}_\ell$ , then our result



in the first multipole bin is altered from  $58.6 \pm 17.3 \mu\text{K}^2$  to a value of  $69.1 \pm 18.5 \mu\text{K}^2$  (95% c.l.).

As a simple consistency check on our calculation, we computed the leftover signal from the difference of the V and W maps, i.e. the power spectrum of a map given by  $\frac{V(\hat{n})-W(\hat{n})}{s_V-s_W}$  and normalized by the beam (the beam is the same to sub-percent level for the two frequency bands at  $\ell < 50$ ), rendering a value of  $697 \mu\text{K}^2$  in the first bin. We subtracted from this quantity the mean simulated noise on the difference map, given by  $\frac{\langle(\sigma_{V;\ell}/b_{V;\ell})^2\rangle+\langle(\sigma_{W;\ell}/b_{W;\ell})^2\rangle}{(s_V-s_W)^2} = 536 \mu\text{K}^2$ . The SZ signal derived from this method is then  $161 \pm 49$  (95% c.l.) in the first bin. This derivation, however, is sub-optimal since it does not fully minimize frequency dependent quantities such as instrumental noise and foregrounds, but only removes common signals like the CMB. Simulations suggest that this method leads to a higher ‘‘SZ’’ signal. Nevertheless this demonstrates that the SZ-like signal we have detected with our optimal method is not associated with a residual CMB that we have not accounted for in simulations related to Table 1.

In binning the SZ spectra into a single multipole bin, we obtain  $\ell(\ell+1)C_\ell/2\pi = 55.1 \pm 15.6 \mu\text{K}^2$  (95% c.l.) for the central multipole of  $\ell = 205$ , which is heavily dominated by the first bin due to its comparatively much tighter error bar. Note that this implies a component with 6% the value of the primordial CMB in the power spectrum (or 24% in  $a\ell m$  temperature). We have failed to find a combination of foreground residuals, beam errors, calibration uncertainty, and similar instrumental systematics that will add up to the needed correction.

As a test on the reliability of the SZ signal detected in the first multipole bin, we varied the foreground model involving the amplitudes of the synchrotron and dust, but within the uncertainties allowed by WMAP data, we failed to find a model that produced a null SZ signal in the first bin. Our error budget includes the full uncertainty in the foregrounds to the extent that foregrounds have been established with WMAP data (Gold et al. 2009). It could be that our signal is a signature of an unknown foreground. If that were to be the case, CMB observations that span a wider range of frequencies will become necessary, and we motivate a study with the on-going Planck experiment.

#### 4. DISCUSSION

If the excess signal we have detected at ten degrees angular scales is indeed SZ, it is clear that the signal does not originate from galaxy clusters at high redshift. Such a signal would lead to a power spectrum that increases with multipoles and we should have detected that SZ signal in our smaller angular scale bins. A large SZ signal associated with the extragalactic sky is also

ruled out by existing arcminute-scale CMB experiments. The only possibility is that the signal is associated with the Galactic halo, perhaps keV to sub-keV gas in the outer skirts and the surrounding region extending to the local group. Such a Galactic signal can naturally explain why the signal is primarily at small multipoles. We can address if such a signal is possible based on requirements on the number density of electrons and the existing constraint on spectral distortion measurement made with FIRAS. Since the SZ effect is  $-2y$  at RJ frequencies, where  $y$  is the Compton  $y$ -parameter, we can convert the amplitude of the fluctuation power, assuming Galactic-like signal with a power-law  $C_\ell \simeq A\ell^{-3}$ , to obtain  $y = (1.9 \pm 0.3) \times 10^{-5}$  (95% c.l.). This is consistent with the 95%-level FIRAS constraint of  $|y| \leq 2.5 \times 10^{-5}$  from the COBE satellite (Mather et al 1994).

The electron column density required to obtain this  $y$ -parameter in our MW halo can be obtained from  $N_e = 2R_{\text{MW}}n_e \simeq \frac{ym_e c^2}{\sigma_T k_B T_e}$ , where  $R_{\text{MW}}$  is the radius of the MW,  $m_e$  is the electron mass,  $T_e$  is the electron temperature, with other constants having the usual definition. For an electron gas temperature of 1 keV, we obtain  $N_e = 1.5 \pm 0.2 \times 10^{22} \text{cm}^{-2}$  (95% c.l.). We note that this column density of free electrons is consistent with the one suggested in Peiris & Smith (2010) to resolve the CMB isotropy anomalies via the kinetic SZ effect. In reality, both the thermal and kinetic SZ effects may contribute to large-scale anomalies of the CMB and whether the dominating effect is kinetic or thermal can be studied with the coming Planck data set, as it provides a map of the CMB at 220 GHz where the SZ thermal signal is expected to disappear. We note that the required column density is in tension with the pulsar dispersion measurements (Taylor & Cordes 1993) which lead to  $N_e \sim 10^{21} \text{cm}^{-2}$ . The pulsar estimate, however, is uncertain due to its assumptions on the metallicity and profile of the hot gas. Moreover, existing pulsars only probe the inner halo and may not probe electrons that span the full extent of our Milky Way halo and beyond. Since the SZ effect is distance independent, electrons that are in the diffuse IGM just outside the halo may be an equal contributor as the electrons just inside the halo. Rather than to simply explain away the signal, as we did not find either a simple statistical argument or systematic effect, we suggest that further studies are warranted on the Galactic SZ signal.

We thank David Buote and Paolo Serra for helpful conversations. S.J. and J.S. acknowledge support from GAANN fellowships from the US Department of Education. This work was also supported by NSF AST0645427 and NASA NNX10AD42G

#### REFERENCES

- Amblard, A. Cooray, A., Kaplinghat, M., Phys. Rev. D **75**, 083508 (2007)  
 Carlstrom, J. E., Holder, G. P., Reese, E. D., Ann. Rev. Astron. Astrophys. **40**, 643 (2002)  
 Cooray, A., Phys. Rev. D **62**, 103506 (2000)  
 Cooray, A., Hu, W., Tegmark, M., Astrophys. J. **540**, 1 (2000)  
 Dawson, K. S., et al., Astrophys. J. **647**, 13 (2006)  
 Dunkley, J., et al. [WMAP Collaboration], Astrophys. J. Suppl. **180**, 306 (2009)  
 Finkbeiner, D. P., Davis, M., Schlegel, D. J., Astrophys. J. **524**, 867 (1999)  
 Finkbeiner, D. P., Astrophys. J. Suppl. **146**, 407 (2003)  
 Fowler, J. W., et al. [ACT Collaboration], arXiv:1001.2934 (2010).

- Friedman, R. B., *et al.* [QUaD collaboration], *Astrophys. J.* **700**, L187 (2009)
- Gold, J. P., Vishniac, E. T., 1986, *ApJ*, 306, L51
- Gold, B., *et al.* [WMAP Collaboration], *Astrophys. J. Suppl.* **180**, 265 (2009)
- Haslam, C. G. T., Stoffel, H., Salter, C. J., Wilson, W. E., *A&AS* **47**, 1 (1982)
- Hill, R. S., *et al.* [WMAP Collaboration], *Astrophys. J. Suppl.* **180**, 246 (2009)
- Hinshaw, G., *et al.* [WMAP Collaboration], *Astrophys. J. Suppl.* **170**, 288 (2007)
- Hivon, E., *et al.* *Astrophys. J.* **567**, 2 (2002)
- Jones, M. *et al.*, 1993, *Nature*, 365, 320.
- Komatsu, E., Kitayama, T., *Astrophys. J.* **526**, L1 (1999)
- Komatsu, E., Seljak, U., *Mon. Not. Roy. Astron. Soc.* **336**, 1256 (2002)
- Komatsu, E., *et al.*, arXiv:1001.4538 [astro-ph.CO].
- Lewis, A., Challinor, A., Lasenby, A., *Astrophys. J.* **538**, 473 (2000) [arXiv:astro-ph/9911177].
- Lueker, M., *et al.* [SPT Collaboration], arXiv:0912.4317 (2009).
- Masi, S., *et al.*, arXiv:astro-ph/0507509.
- Mather, J. C., *et al.*, *Astrophys. J.* **420**, 439 (1994).
- Molnar, S. M., Birkinshaw, M., *Astrophys. J.* **537**, 542 (2000)
- Nolta, M. R., *et al.* [WMAP Collaboration], *Astrophys. J. Suppl.* **180**, 296 (2009)
- Ostriker, J. P., Vishniac, E. T., 1986, *ApJ*, 306, L51
- Page, L., *et al.* [WMAP Collaboration], *Astrophys. J. Suppl.* **170**, 335 (2007)
- Peiris, H. V., Smith, T. L., arXiv:1002.0836v1 (2010).
- Reichardt, C. L., *et al.*, *Astrophys. J.* **694**, 1200 (2009)
- Sadeh, S., Rephaeli, Y., *New Astron.* **9**, 373 (2004)
- Sayers, J., *et al.*, *Astrophys. J.* **690**, 1597 (2009)
- Seljak, U., Burwell, J., Pen, U. L., *Phys. Rev. D* **63**, 063001 (2001)
- Sievers, J. L., *et al.*, arXiv:0901.4540 [astro-ph.CO].
- Sharp, M. K., *et al.*, arXiv:0901.4342 [astro-ph.CO].
- Springel, V., White, M. J., Hernquist, L., arXiv:astro-ph/0008133.
- Sunyaev, R. A., Zeldovich, Y. B., *Comments Astrophys. Space Phys.* **4**, 173 (1972).
- Taylor, J. H., Cordes, J. M., *Astrophys. J.* **411**, 674 (1993).
- Tegmark, M., Efstathiou, G., arXiv:astro-ph/9507009.
- Tegmark, M., de Oliveira-Costa, A., Hamilton, A., *Phys. Rev. D* **68**, 123523 (2003)
- Veneziani, M., *et al.*, *Astrophys. J.* **702**, L61 (2009)